Modeling Solute Diffusion in the Presence of Pore-Scale Heterogeneity

Sean W. Fleming
Department of Geosciences
104 Wilkinson Hall, Oregon State University, Corvallis, OR 97331-5506

current address:
Waterstone Environmental Hydrology and Engineering, Inc.
1650 38th St., Suite 201E, Boulder, CO 80301
e-mail: fleming_sean@hotmail.com

*** Roy Haggerty**
Department of Geosciences
104 Wilkinson Hall, Oregon State University, Corvallis, OR 97331-5506
e-mail: haggertr@geo.orst.edu
telephone: (541) 737-1210

* corresponding author

Submitted to
Journal of Contaminant Hydrology
August 10, 1999

key words: *diffusion model, multirate, rate-limited mass transfer, Culebra, contaminant transport, dolomite*

DISCLAIMER

Modeling Solute Diffusion in the Presence of Pore-Scale Heterogeneity

Sean W. Fleming[1, 2] and Roy Haggerty[1, 3]

ABSTRACT

A range of pore diffusivities, D_p, is implied by the high degree of pore-scale heterogeneity observed in core samples of the Culebra (dolomite) Member of the Rustler Formation, NM. Earlier tracer tests in the Culebra at the field-scale have confirmed significant heterogeneity in diffusion rate coefficients (the combination of D_p and matrix block size). In this study, expressions for solute diffusion in the presence of multiple simultaneous matrix diffusivities are presented and used to model data from eight laboratory-scale diffusion experiments performed on five Culebra samples. A lognormal distribution of D_p is assumed within each of the lab samples. The estimated standard deviation (σ_d) of $\ln(D_p)$ within each sample ranges from 0 to 1, with most values lying between 0.5 and 1. The variability over all samples leads to a combined σ_d in the range of 1.0 to 1.2, which appears to be consistent with a best-fit statistical distribution of formation factor measurements for similar Culebra samples. A comparison of our estimation results to other rock properties suggests that, at the lab-scale, the geometric mean of D_p increases with bulk porosity and the quantity of macroscopic features such as vugs and fractures. However, σ_d appears to be determined by variability within such macroscopic features and/or by micropore-scale heterogeneity. In addition, comparison of these experiments to those at larger spatial scales suggests that increasing sample volume results in an increase in σ_d.

[1] Department of Geosciences, 104 Wilkinson Hall, Oregon State University, Corvallis, OR 97330-5506
[2] Now at: Waterstone Environmental Hydrology and Engineering, Inc., 1650 38th St., Suite 201E, Boulder, CO 80301
[3] Corresponding author; e-mail: haggertr@geo.orst.edu, telephone: (541) 737-1210

1. INTRODUCTION

Mass transfer refers to the movement of a constituent from one phase or region to another along a concentration gradient (e.g., *Welty et al., 1984*). In the context of solutes in geologic materials, this involves movement of solute from pores dominated by advection (advective porosity) into dead-end pores dominated by diffusion (diffusive porosity) or onto sorption sites on the surface of grains. This phenomenon has two well-known and significant implications for solute transport in groundwater. First, the rate of advective transport away from the source decreases through time as the solute spends less time in advective porosity and more time in diffusive porosity containing stagnant water (e.g., *Roberts et al., 1986; Quinodoz and Valocchi, 1993*). This phenomenon partly determines how far and how fast a solute will be transported, and is particularly important to evaluation of the environmental risk involved in geologic disposal of nuclear waste. Secondly, remediation of a contaminated aquifer by pump-and-treat, soil vapor extraction, and bioremediation techniques is slowed if mass transfer from diffusive to advective porosity is rate-limited (*Steinberg et al., 1987; Brusseau and Rao, 1989; Goltz and Oxley, 1991; Gierke et al., 1992; Armstrong et al., 1994; Fry and Istok, 1994; Harvey et al., 1994; Rabideau and Miller, 1994; Haggerty and Gorelick, 1995*). Diffusion in geologic media also has implications for petroleum migration (e.g., *Mann, 1994*), evaluation of residual oil saturation in hydrocarbon reservoir studies (e.g., *Tomich et al., 1973; Deans and Carlisle, 1986*), determination of $^{40}Ar/^{39}Ar$ cooling histories in geochronology studies (*Lovera et al., 1989; Lovera et al., 1993*), and evaluation of the relationship between fluid and melt inclusions and magma chemistry (*Qin et al., 1992*).

A simplifying assumption made in most treatments of nonequilibrium mass transfer in geologic media is that a single rate of sorption or diffusion is present. The implication of this assumption is that rock is homogeneous, or can be treated as effectively homogeneous at the spatial scale of interest. However, most rock is not homogenous at the spatial scales at which mass transfer processes operate. In the context of lab-scale diffusion, this heterogeneity may result from variability

in the volume, size, and geometry of macroporosity or microporosity in aquifer particles and aggregates of particles (*Rao et al., 1980; Pignatello, 1990; Wood et al., 1990; Ball and Roberts, 1991; Harmon et al., 1992; Harmon and Roberts, 1994*) and the external and internal geometry of small lenses of impermeable material, and the proportion of this material (*Shackelford, 1991*). As these factors control rates of matrix diffusion, and as they are heterogeneous at the pore scale, diffusion should also be heterogeneous at the pore scale. That is, in a given volume of rock, multiple rates of diffusion occur simultaneously, and "multirate" mass transfer may therefore be needed to adequately describe solute transport (e.g., *Villermaux, 1981; Pedit and Miller, 1994; Haggerty and Gorelick, 1995*). The effects of multirate mass transfer have been measured in lab-scale soil column experiments (e.g., *Ball and Roberts, 1991; Grathwohl and Kleineidam, 1995; Pedit and Miller, 1995; Culver et al., 1997; Werth et al., 1997; Haggerty and Gorelick, 1998; Rügner et al., 1999*) and more recently in integrated and comprehensive field-scale studies of the transport properties of the Culebra dolomite at the Waste Isolation Pilot Plant (WIPP) site (*Meigs and Beauheim, in review; Haggerty et al., in review; McKenna et al., in review*).

The WIPP is a proposed repository for defense-generated transuranics located about 20 miles northeast of Carlsbad, New Mexico (Figure 1). The Culebra Member of the Rustler Formation, a Permian evaporitic dolomite, is considered to be the most transmissive laterally continuous hydrogeologic unit in the WIPP area and the most likely pathway of radionuclide transport from the repository in the event of human intrusion (*Holt, 1997; Meigs and Beauheim, in review*). Due to a complex history of deposition, diagenesis, and fracturing (see *Holt, 1997* for a review), the Culebra dolomite is characterized by a high degree of lithologic and structural heterogeneity (Figure 2). Detailed analysis of core has clearly revealed multiple scales of fracturing, along with spatially variable amounts of vuggy porosity and gypsum-filling of vugs and fractures; poorly cemented, silt-size dolomite interbeds are also common (*Holt, 1997*). The presence of multirate diffusive mass transfer in the Culebra, at both lab- and field-scales, has been inferred from this observed heterogeneity (*Holt,*

1997), and its effects at the field-scale have been confirmed by suites of tracer tests at two locations (*Meigs and Beauheim, in review; Haggerty et al., in review; McKenna et al., in review*).

Our objectives in this paper are (1) to formulate a mathematical model of diffusion in a rock with variable diffusivity; (2) to solve the resulting mathematical equations; and (3) to estimate distributions of diffusivities from a suite of laboratory diffusion experiments performed upon the Culebra dolomite.

2. DIFFUSION EXPERIMENTS AND DATA

Data obtained from static diffusion experiments conducted by Sandia National Laboratories (*Tidwell et al., in press*) were analyzed in this study. The x-ray imaging technique used in these experiments is described in *Tidwell and Glass* (*1994*), and details of the sample selection, experimental set up, and results are given in *Christian-Frear et al.* (*1997*) and *Tidwell et al.* (*in press*); a brief overview is given here. Five small (approximately 6 cm by 4 cm by 2.5 cm thick) rectangular blocks of Culebra core were selected to represent a range of Culebra porosity types (see Figure 2 and Table 1). Because of limitations on sample availability, samples with significant interparticle porosity (silty dolomite, which is not uncommon in the Culebra) could not be represented among the samples. The samples were attached to a constant-concentration tracer reservoir at one end and sealed along their other edges to form no-flux boundaries. Constant concentration was maintained within 1% of a target concentration by slow circulation in the tracer reservoir. The tracer consisted of potassium iodide (KI), dissolved in a sodium chloride (NaCl) solution simulating naturally-occurring Culebra pore fluids (brine). Each block was initially saturated with brine. Tracer was then allowed to diffuse from the reservoir into the sample (in-diffusion). At the end of the in-diffusion experiment, a head gradient was established across the block and tracer was forced across it until the KI concentration within the pore space was equal to that in the reservoir (i.e., until the sample was completely flushed with the KI solution). The reservoir fluid was then replaced with pure NaCl solution, and the tracer

within the block was permitted to diffuse back out into the reservoir (out-diffusion). Slow circulation of fluids through the reservoir was again performed to maintain concentrations within 1% of the target concentration.

X-ray images of each block were taken at intervals during the in- and out-diffusion experiments (*Tidwell et al., in press*). As the presence of the iodide ion alters the amount of x-ray energy transmitted through the sample, these images provide maps of porosity and of normalized KI concentration in the rock through time. The images were then further processed to provide the normalized mass uptake and recovery data used in our modeling (Figure 3).

Three important difficulties were encountered during the course of the experiments. First, tracer concentration in the reservoir was accidentally varied during the earliest phases of the in-diffusion study, resulting in a time-varying boundary condition. Second, sufficient dissolution of pore-filling gypsum in sample RC6-G occurred during the course of the experiment that its porosity was significantly increased; this block was omitted from the out-diffusion experiment. Lesser gypsum dissolution also took place in sample B33-H. In both cases, this probably occurred while the sample was being saturated with KI tracer in preparation for the out-diffusion phase (*V. Tidwell, personal communication, 1998*). Third, it proved impossible to fully saturate sample RC4-D with tracer, so it was also omitted from the out-diffusion phase.

In addition to examining each data set separately, we combined the data from individual samples to form bulk in- and out-diffusion data sets. The bulk data are what would be obtained experimentally if all the samples were joined together in parallel along a single reservoir, and normalized mass diffused in or out was measured for all blocks at once using a single x-ray image. This was done for the purpose of obtaining a rough approximation to diffusion in a larger, more heterogeneous volume of Culebra. It is important to re-emphasize, however, that the samples examined do not represent the full lithologic variability within the Culebra. The bulk mass ratio curve we obtained is the arithmetic mean of the individual mass ratio curves, weighted by the sizes of the samples. Use of the bulk diffusion data sets is intended to simulate a larger-scale scenario in

which an extended reservoir of solute (e.g., an advective flow pathway) encounters a variety of matrix types, as represented by the different blocks of varying porosity scales and types (Figure 2 and Table 1) used in the diffusion experiments.

3. MATHEMATICAL AND CODE DEVELOPMENT

Here we present expressions describing one-dimensional diffusion into or out of a rock matrix in the presence of both uniformity and heterogeneity in D_p. Consider a sample of Culebra dolomite of bulk porosity, θ, bounded at one end by a reservoir of solute (potassium iodide in our case) with a time-varying concentration, bounded at the other end by a no-flux boundary, and having an arbitrary but uniform initial solute concentration. Conventional, single-rate diffusion (i.e., a single diffusivity) of KI tracer into or out of the pore space of the sample is described by the diffusion equation:

$$\frac{\partial C}{\partial t} = D_p \frac{\partial^2 C}{\partial x^2} \qquad (Eqn.\ 1a)$$

where C is the concentration of solute within the pore space [M/L^3, or dimensionless if normalized], and D_p is the pore diffusivity [L^2/T], which is some fraction of the aqueous diffusivity of the solute in water, D_{aq} [L^2/T]. The boundary and initial conditions are:

$$C(x = l, t) = C_1(t) \qquad (Eqn.\ 1b)$$

$$\frac{\partial C(x = 0, t)}{\partial x} = 0 \qquad (Eqn.\ 1c)$$

$$C(x, t = 0) = C_0 \qquad (Eqn.\ 1d)$$

where C_0 is the initial concentration in the sample [M/L³]. A simple expression for D_p is (e.g., *Bear, 1972*):

$$D_p = \tau D_{aq} \qquad (Eqn.\ 2)$$

where τ, the tortuosity [-], is defined as l^2/L^2 (e.g., *Bear, 1972*); l is the straight-line distance from one end of the pore to the other [L] and L is the actual length along the winding pore [L]; and $l^2/L^2 < 1$. D_p may be reduced if sorption occurs within the pore, or if restrictivity is significant (i.e., if the pore radius is similar to the ionic or molecular radius of the solute; e.g., *Satterfield et al., 1973*). For a complete review of the theory of diffusion in rock, see *Ohlsson and Neretnieks (1995)*.

Taking the Laplace transforms of Eqns. 1.a-c simplifies the diffusion equation to a second-order nonhomogeneous ordinary differential equation:

$$\frac{\partial^2 \overline{C}}{\partial x^2} - \frac{p}{D_p}\overline{C} = \frac{-C_0}{D_p} \qquad (Eqn.\ 3.a)$$

where $\overline{C}$ is the Laplace transform of concentration within the pore space and p is the Laplace parameter. The boundary conditions are now:

$$\frac{\partial \overline{C(x=0)}}{\partial x} = 0 \qquad (Eqn.\ 3.b)$$

and:

$$\overline{C(p, x=l)} = \overline{C_1(p)} \qquad (Eqn.\ 3.c)$$

Solving Eqn. 3.a subject to Eqns. 3.b and c by the method of undetermined coefficients gives:

$$\overline{C(p,x)} = \left[\overline{C_1(p)} - \frac{C_0}{p}\right]\left[\frac{e^{x\sqrt{p/D_p}} + e^{-x\sqrt{p/D_p}}}{e^{l\sqrt{p/D_p}} + e^{-l\sqrt{p/D_p}}}\right] + \frac{C_0}{p} \qquad (Eqn.4)$$

The 0th spatial moment of the concentration profile gives a measure of the solute mass, $M(t)$, within the slab at time, t:

$$M(t) = \theta A \int_{x=0}^{x=l} C(x,t)dx \qquad (Eqn.5)$$

where A is the cross-sectional area of rock exposed to the solute reservoir, and which is required if $C(x,t)$ is given conventional (three-dimensional) units of mass/unit volume. Taking advantage of the fact that the Laplace transform is a linear operator, substituting Eqn. 4 into Eqn. 5, integrating, and recognizing the definition of the hyperbolic tangent gives the following expression for diffusive mass uptake or release in the presence of uniform D_p subject to the boundary and initial conditions encountered in the static diffusion experiments: .

$$M(t, D_p) = (\theta A) L^{-1}\left\{\left[\frac{\overline{C_1(p)} - \frac{C_0}{p}}{\sqrt{p/D_p}}\right] Tanh(l\sqrt{p/D_p}) + \frac{C_0 l}{p}\right\} \qquad (Eqn.6)$$

where the symbol L^{-1} indicates the inverse Laplace transform. Eqn. 6 and the inverse Laplace transform of Eqn. 4 are generally useful solutions to the diffusion equation, as they can

accommodate any initial concentration and a constant or time-varying boundary concentration. For notational convenience later in the derivation, we define $M'(t,D_p)$ thusly:

$$M'(t,D_p) = M(t,D_p)/\theta \qquad (Eqn.\,7)$$

Now consider a model of pore-scale heterogeneity in which porosity in the rock matrix consists of many 1-D, non-intersecting pores. The pore diffusivity is constant along the length of each pore but may be different between neighboring pores. Changes in pore diffusivity are due, at a minimum, to differing tortuosity and cross-sectional area of the pores. Although the pores do in fact intersect, the assumption of many 1-D, non-intersecting pores allows us to retain the simplicity of 1-D diffusion while incorporating the significant effects of variable diffusivity. Approaches similar to this have previously been successfully used to accommodate the effects of variable diffusivity upon solute transport (e.g., *Cunningham et al.*, 1997; *Haggerty and Gorelick*, 1998; *Haggerty et al., in review*).

The total mass diffused into the pore space at a given time is the sum of the contributions to diffusive mass uptake or release of the different values of D_p present in the rock. For the case of a continuous distribution of D_p, total mass uptake or release for the sample is described by the following expression (*Fleming, 1998*):

$$M(t) = \theta \int_a^b f_c(D_p) M'(t,D_p)\, dD_p \qquad (Eqn.\,8)$$

where the integration limits, a and b represent the minimum and maximum possible values of D_p and may be taken in general to be 0 and ∞; and $f_c(D_p)$ is a density function (DF) which describes the relative frequencies of different values of D_p in terms of the proportion of the total porosity in which those values of D_p are operative:

$$f_c(D_p) = \frac{\partial}{\partial D_p}\left(\frac{\theta_{D_p}}{\theta}\right) \qquad (Eqn.\,9)$$

where θ_{Dp}/θ is the ratio of the porosity constituted by pores with a particular pore diffusivity, D_p, to the total porosity of the sample. It is important to note that the use of a DF does not imply that D_p is stochastic. Rather, the function $f_r(D_p)$ is simply a means of weighting the contribution, $M'(t,D_p)$, to total mass uptake or release, $M(t)$, made by a particular pore diffusivity, D_p, on the basis of the relative (volumetric) prevalence of pores with that value of D_p. The full derivation is given in *Fleming (1998)*, but note that Eqn. 8 is very similar in form to an expression presented in the chemical engineering literature over a quarter of a century ago which quantified diffusive mass uptake in the presence of a continuous distribution of grain sizes (*Ruthven and Loughlin, 1971*).

The function $f_r(D_p)$ may be any continuous distribution. A number of general considerations suggest that a lognormal distribution may be appropriate (*Haggerty and Gorelick, 1998*). Discrete distributions and alternative continuous DFs have also been used, such as gamma and piece-wise linear distributions (see *Hollenbeck et al., 1999*). However, formation factor data from the Culebra dolomite support the assumption of a lognormal DF (Figure 4), and previous analyses of tracer tests performed in the Culebra obtained excellent results using a lognormal distribution (*Haggerty et al., in review; McKenna et al., in review*).

We normalize $M(t)$ by the maximum total solute mass present in the rock, M_T. In the case of diffusion into the rock, this is the mass at $t = \infty$. For diffusion out of the rock, this is the mass at $t = 0$. This maximum total mass is given by:

$$M_T = \theta A l C_E \qquad (Eqn.10)$$

where the l is the length of the rock slab as measured away from the reservoir and C_E is the initial sample concentration out-diffusion (C_0) and the late-time sample concentration for in-diffusion ($C(t=\infty)$). If normalized concentrations are used, $C_E = 1$.

Making the appropriate substitutions for $f_d(D_p)$ and $M'(t,D_p)$ into Eqn. 8 and normalizing by Eqn. 10 yields:

$$\frac{M(t)}{M_T} = \frac{1}{l C_E} \int_a^b \left\{ \left(\frac{1}{\sqrt{2\pi} D_p \sigma_d} e^{-\frac{1}{2\sigma_d^2}[\ln(D_p) - \mu_d]^2} \right) L^{-1} \left\{ \left[\frac{\overline{C_1(p)} - \frac{C_0}{p}}{\sqrt{p/D_p}} \right] Tanh(l\sqrt{p/D_p}) + \frac{C_0 l}{p} \right\} dD_p \right\} \quad (Eqn. 11)$$

where μ_d and σ_d are the mean and standard deviation, respectively, of $\ln(D_p)$.

A FORTRAN77 code was written to solve Eqn. 11 for both forward simulation and parameter estimation. The purpose of the code was to obtain estimates of the values of μ_d and σ_d from the diffusion data previously discussed. Note that a distribution of diffusivities interpreted from data under the assumption of nonintersecting pores in a parallel arrangement, aligned approximately normal to the surface of the sample, should be considered a lumped distribution representing what may be diffusion in parallel and series in a more complex geometry (*Haggerty and Gorelick, 1998*). Several subroutines from the IMSL (International Mathematics and Statistics Libraries) Version 3.0 package were used. These subroutines use the de Hoog algorithm to numerically evaluate the inverse Laplace transform (*de Hoog et al., 1982*), Gauss-Kronrod rules to perform numerical integration, and a modified Levenberg-Marquardt algorithm (*Marquardt*, 1963) and a finite-difference Jacobian to solve the nonlinear least-squares optimization problem. The lower and upper limits of integration were set to the 1×10^{-7} and $(1 - 1\times10^{-7})$ percentile values of D_p, respectively, for a given μ_d and σ_d. For large values of the Laplace parameter, p, the complex value of the hyperbolic tangent in Eqn. 11 was set to [1,0] to overcome numerical difficulties (*Fleming, 1998*). Capability to use Eqns. 6 and 10 to estimate a conventional, single-rate diffusivity from the normalized mass data was also incorporated into the code.

Log-space root mean square error (RMSE) was used as a measure of fit, as log-transformed data shows a greater sensitivity to the late-time, low mass ratios at which multirate effects are greatest (e.g., *Ruthven and Loughlin, 1971; Haggerty and Gorelick, 1998*). Similar concerns led us to convert the in-diffusion mass ratio curves, which are large-valued at late times, to:

$$1-\frac{M(t)}{M_T} \qquad (Eqn.12)$$

which is small-valued at late times. This approach was also used by *Ruthven and Loughlin (1971)*. When the data is then log-transformed, small relative changes in the raw late-time mass ratio data give rise to significantly larger relative changes in the converted and transformed values.

An approximation of parameter estimation statistics are calculated using the Jacobian, or sensitivity, matrix. This is a n by nt matrix, where n is the number of parameters to be estimated (1 for a single-rate model, 2 for multirate) and nt is the number of data points in the mass ratio curves. The entries of the Jacobian, J_{ij}, consist of the derivative of the calculated mass ratio at the i^{th} time, M_i/M_T, with respect to the j^{th} parameter, p_j (e.g., *Knopman and Voss, 1987; Harvey et al., 1996*):

$$J_{ij} = \frac{\partial\left(M_i/M_T\right)}{\partial p_j} \qquad (Eqn.13)$$

The covariance matrix is a n by n matrix estimated by taking the inverse of the square of the Jacobian and multiplying each entry by the variance of the random error in the observed data (e.g., *Knopman and Voss, 1987*). As we have no direct measure of the error in the data, we follow the common approach [e.g., *Bard, 1974*, p. 178] of using the mean square error between the data and the calculated curves as a surrogate for the replicate variance. The square roots of the entries along the diagonal of the covariance matrix give, in turn, the standard deviations (68% confidence intervals) of normally-distributed error about the best-fit values of the estimated parameters. Our code returned estimates

of the arithmetic value of μ_d but of the natural logarithms of D_p and σ_d, so in arithmetic space the confidence intervals are symmetric about μ_d but asymmetric about D_p and σ_d.

4. RESULTS

Suites of forward simulations demonstrating the effects of variation in μ_d and σ_d, and comparing single-rate diffusion to multirate diffusion, are given in Figure 5. Plots of the static diffusion data and of curves calculated using best-fit single-rate and multirate models are given for two examples in Figure 6. Table 2 summarizes the results for all experiments, giving the best-fit value of D_p for each sample and for bulk diffusion obtained using a single-rate model, as well as the corresponding best-fit multirate parameters. Larger μ_d values indicate faster diffusion, on average, for a given block length and larger σ_d values indicate the presence of a wider range of D_p (i.e., more significant multirate effects). RMSE values are also given, as are estimates of 95% confidence intervals for D_p, μ_d, and σ_d.

While the quality of the fits of the calculated curves to the data is generally good, these matches are inferior to those obtained from analysis of field-scale Culebra tracer tests using a multirate mass transfer model (*Haggerty et al., in review; McKenna et al., in review*) and to those obtained from other laboratory data where multirate mass transfer was investigated (e.g., *Werth et al.*, 1997; *Haggerty and Gorelick*, 1998). This is attributed to a combination of the quality of our data and model assumptions that may not be fully valid. The scatter apparent in Figures 3 and 6 may result from some combination of failure to maintain a constant-concentration boundary condition, gypsum dissolution, and a lack of precision in the x-ray imaging technique, which is still under development. Our assumption of constant diffusivity along the pore, though also assumed in other studies of this type, is likely a poor assumption for a small sample of the Culebra dolomite, which is highly heterogeneous at all spatial scales. The assumptions of purely one-dimensional diffusion and of a lognormal distribution of diffusivity are potentially in error, particularly in samples that may be

dominated by a small number of porosity types (for example, fractures and intragranular porosity). The model used in this paper is best applied when the averaging volume is large relative to the scale of heterogeneity; this condition is probably not met within some of the individual samples we examined.

Since D_{aq} increases somewhat with concentration (see *Cussler, 1997*), variation in tracer concentration within the samples with time might have led to changes in D_p over the course of the experiment. However, *Cussler (1976)* showed that concentration-dependence of D_{aq} has a negligible effect on concentration profiles and breakthrough curves in systems similar to the static diffusion experiments. As the mass ratio curves used in our analysis are integrated concentration curves, concentration-dependent D_{aq} should not be a significant source of error. Moreover, we were permitted to test whether this was an important effect by noting that the average tracer concentration within a given sample was significantly higher during the out-diffusion phase than during in-diffusion. If concentration-dependence of D_{aq} was present and had a significant effect upon the mass curves, then the out-diffusion experiments would give consistently larger diffusivities than those obtained with the same sample from the in-diffusion experiments. This was not observed (Table 2).

Comparison of D_{aq} of the KI tracer to the best-fit distribution of pore diffusivities (for the multirate model) and the best-fit D_p (for the single-rate model) might provide a means of confirming the reasonableness of the parameter estimates, because D_p can never exceed D_{aq}. However, three considerations show that such comparisons are both problematic and unnecessary. First, although D_p and μ_d are well-constrained, the confidence intervals about the best-fit values are nonetheless sufficiently wide (largely due to data scatter) to accommodate any reasonable value of D_{aq} for this system. Second, judging the entire distribution against D_{aq} presumes that the tails of the distribution should be reliable. However, the lognormal distribution is only an approximation to the true distribution of diffusivities in the rock. Moreover, the sensitivity of any experiment to diffusion rates in the tails of the distributions is lower than that to rates of diffusion closer to the mean (*Haggerty et*

al., in review). Third, D_{aq} is unknown for these experiments, which consisted of a quaternary diffusion system containing Na^+, Cl^-, K^+, and I^- ions. Some other species might also have been present, such as calcium and sulfate ions produced by gypsum dissolution. The complexities of multicomponent diffusion are discussed in detail in *Cussler (1997)* and *Fleming (1998)*; essentially, D_{aq} must be determined experimentally, which has not been done for this diffusion system.

5. DISCUSSION

5.1 Single-Rate versus Multirate Models

The 95% confidence ranges in σ_d for B33-H, RC1-A, and RC4-D do not include 0 (Table 2). It is also clear from the $RMSE_{MR}$ and $RMSE_{SR}$ values that the multirate model provides a quantifiably superior fit. Multirate diffusion, therefore, occurs in these samples. In contrast, conservative consideration of the in-diffusion and out-diffusion results taken together suggests that multirate diffusion was not detected in samples RC2-B and RC6-G.

Multiple simultaneous diffusivities are significant at the lab-scale in spite of the relatively small estimated values of σ_d and the fact that two of the five samples can not be proven to show multirate effects from our modeling of this data. There are three reasons for this. First, the assumed distribution is lognormal, so a relatively small σ_d represents significant variability in D_p. A σ_d value of 0.5, for example, indicates almost an order of magnitude difference between the 0.025 and 0.975 quantile diffusivities. This difference increases to a factor of 50 for a σ_d of 1.

Second, while the visible effects of variable diffusivity upon the mass ratio curves generally do not appear to be large for small values of σ_d (Figure 6), single-rate and multirate curves diverge at later times (Figure 5; see also *Ruthven and Loughlin, 1971; Haggerty and Gorelick, 1998*). This is consistent with the finding by *Cunningham and Roberts* (1998) that even small variability in diffusivity may have significant implications for long-term solute transport.

Third, we conservatively rejected the hypothesis that a range of diffusivity is present in a given sample if we could not prove that it was. If the 95% confidence range in estimated σ_d included or very nearly included 0, and if the RMSE values did not show that the multirate model provided a significantly better fit than the single-rate model, it was concluded that multirate diffusion was not present. However, these tests do not indicate that a single-rate model is preferred, either. Any σ_d range which included 0 also included infinity; the inversion statistics in such a case indicate that it is impossible to determine from the available data whether multirate effects are present in that sample. This is due to a high degree of insensitivity of RMSE, over the dynamic range of the data, for a given value of μ_d (which is reasonably well-estimated in all cases), and in the presence of scatter in the data, to the value of σ_d. If a single-rate model was clearly superior, the multirate inversion would return a value of σ_d near 0 with narrow confidence bounds. Data collection to later times (i.e., over a greater dynamic range) might facilitate far more reliable estimates of σ_d (Figure 5).

Work by *Tidwell et al. (in press)* detected variability in diffusivity in samples RC2-B and RC6-G (for example, RC2-B contains a fracture), whereas our modeling did not. *Tidwell et al. (in press)* analyzed concentrations along parallel transects into the samples, whereas we analyzed the mass in the whole sample through time. This whole-sample mass measurement is influenced by multirate diffusion in approximately the same manner as a tracer test along a fracture through the rock would be influenced, insofar as a tracer test samples all of the diffusivities simultaneously. In addition, both whole-sample mass measurements and solute tracer tests are most strongly influenced by small amounts of rock with lower-than-average diffusivities (e.g., *Cunningham and Roberts*, 1998), whereas the fracture contained in RC2-B has a higher-than average diffusivity. The results obtained using whole-sample mass measurements are thus more amenable to comparison with previous, field-scale results. It is also important to recall that our results do not preclude the presence of multirate effects in these two samples, as explained previously.

The bulk diffusion data clearly show multirate effects, as expected (see Table 2). In addition, some of the key characteristics of the bulk diffusion can be assembled from diffusion in the

individual samples. Using in-diffusion as an example, the geometric mean of the estimated D_p values for the individual blocks (2.27 x 10^{-6} m^2/hr) is very similar to the estimated geometric mean of the lognormal distribution for the bulk data (2.26 x 10-6 m^2/hr). In addition, the minimum estimated value of D_p for an individual block (RC4-D, 9.57 x 10^{-7} m^2/hr) corresponds roughly to the 20th percentile in the lognormal CDF of diffusivities (9.96 x 10^{-7} m^2/hr). Similarly, the maximum estimated value of D_p for an individual block (B33-H, 4.78 x 10^{-6} m^2/hr) corresponds roughly to the 80th percentile in the lognormal CDF of diffusivities (5.16 x 10^{-6} m^2/hr). Of course, neither the five single-rate D_p values nor the five lognormal distributions from the individual slabs combine additively, in a rigorous sense, to form a new lognormal distribution corresponding to the bulk experiment. However, it is clear that the estimated lognormal distribution estimated solely from the bulk diffusion data provides a reasonable representation of the range of pore diffusivities known to exist within the individual slabs. Again we note that the bulk diffusion data do not represent the full lithologic variability within the Culebra, and therefore our results should not be taken to represent the full variability of diffusivity within the Culebra.

5.2 Diffusivity and Formation Factor

As diffusivity is inversely proportional to formation factor, the distribution of one should be similar to that of the other. Unfortunately, calculation of absolute D_p values from formation factor data may be unreliable and it is therefore difficult to directly convert a CDF of formation factors to a CDF of D_p. However, the standard deviation of the best-fit lognormal distribution of formation factors determined from all 21 Culebra samples (see Figure 4 and caption) should be similar to σ_d estimated from the bulk static diffusion experiments. σ for the formation factors was found to be approximately 0.7, which is similar to the values found for bulk diffusion data. This reasonably close correspondence serves as supporting evidence for our interpretation of the diffusion experiments, and raises the possibility that formation factors – which are much easier and cheaper to obtain than

laboratory diffusion data – might provide an indirect but reasonably reliable means of estimating pore-scale heterogeneity.

5.3 Other Implications:

It is useful to compare diffusion parameters with conventional descriptions of geologic media. Our ability to determine firm correlations is currently limited by the small number of samples and the large confidence bounds on σ_d. Nonetheless, it appears that μ_d increases with bulk porosity and the relative presence of certain macroscopically visible features (fracturing, vugginess, and gypsum-filling), whereas σ_d does not appear to correlate with these parameters or the number of different types of features present in a given sample (*Fleming, 1998*). Greater interconnectedness of the pore space due to increased porosity and increased presence of large porosity features likely leads to faster average rates of diffusion relative to dead-end pores in which solute becomes trapped (e.g., *Dykhuizen and Casey, 1989*). Gypsum occurs in the Culebra within vugs and fractures (*Holt, 1997*), and may simply be an indicator of interconnected fracture and vug porosity. The apparent lack of correlation between σ_d and macroscopically visible features suggests that σ_d may be controlled by variability in pore geometry within these features and/or by micropore-scale (intergranular or intercrystalline) porosity variability.

Another motivation for laboratory-scale studies was to evaluate whether spatial scaling relationships might exist. Comparison of best-fit σ_d values from experiments at three spatial scales (individual samples, bulk diffusion, and the results of previous field-scale tracer tests) suggests that σ_d increases with sampling volume (*Fleming, 1998*). In our work on sample volumes in the range of 60 to 70 cm^3, the estimated value of σ_d is 0 to 1. The bulk diffusion data have a combined sample volume of 3.3×10^2 cm^3 and have an estimated σ_d of 1 to 1.2. Single-well injection-withdrawal tests conducted at the same location as the samples were taken from [*Meigs and Beauheim, in review*] had

sample volumes of 2×10^{-2} m^3 to 3×10^{-2} m^3. *Haggerty et al.* [*in review*] estimated σ_d on diffusion rate coefficients in these tests in the range of 2.5 to 7. Two-well tracer tests conducted at the same site [*McKenna et al., in review*] on slightly larger sample volumes had estimated σ_d values of 5.5 [*McKenna et al., in review*], although a single-rate model also provided a good representation of the data. We note that the estimates of σ_d at the field-scale also incorporate the effects of variability in block-size in addition to variability in D_p.

The basic physical reasons for increasing σ_d with sample volume are fairly clear. In general, geologic materials are heterogeneous in most respects, and a greater range in the property of interest is commonly found if a larger region is considered. As σ_d is a measure of heterogeneity in D_p within the volume of rock sampled, it may increase as that sampling volume increases and a wider range of D_p is thus encountered. However, at least three conditions preclude determination of a quantitative relationship between spatial scale and mass transfer at this time: (1) the small number of sampling volumes for which Culebra mass transfer data are available (2) the samples used in the laboratory diffusion experiments do not fully reflect the range of lithologies in the Culebra; (3) the uncertainty in block-size variability at the field-scale, the effects of which cannot currently be separated from variability in D_p.

6. CONCLUSIONS

An expression for solute diffusion in the presence of multiple simultaneous matrix diffusivities, D_p, was developed. This was then used to model data from eight laboratory-scale diffusion experiments performed on five core samples (approximately 5 cm by 4 cm by 2.5 cm) of the Culebra Member of the Rustler Formation, a heterogeneous, fractured, evaporitic dolomite. A lognormal distribution of D_p was assumed.

Our main conclusions are: (1) The estimated standard deviation (σ_d) of $\ln(D_p)$ within each Culebra dolomite sample ranges from 0 to 1. Most values lie between 0.5 and 1, implying at least half

an order of magnitude variation in D_p within each small sample; and (2) The variability over all samples leads to a combined σ_d in the range of 1.0 to 1.2, which appears to be consistent with both diffusion results from the individual samples and a best-fit statistical distribution of formation factor measurements for similar Culebra samples. The high observed degree of variability in mass transfer rates within even such small volumes as these is of considerable significance to groundwater remediation and geologic waste disposal issues.

Inferences with respect to geologic controls upon multirate mass transfer parameters should be regarded as tentative at this time due to limited data availability. Nonetheless, important preliminary conclusions in this regard, which should serve as a focus for future investigations, include the following: (3) Comparison of our estimation results to other rock properties suggests that, at the lab-scale, the geometric mean of D_p increases with bulk porosity and the prevalence of macroscopic porosity features such as fractures and vugs. This is attributed to increases in the interconnectedness of the pore space; and (4) Comparison of our results with experiments at larger spatial scales suggests that increasing sample volume results in an increase in σ_d. The value of σ_d does not appear to be correlated to bulk porosity or the prevalence of macroscopic porosity features, but may be determined by variability within such macroscopic features and/or by micropore-scale heterogeneity.

ACKNOWLEDGEMENTS

We wish to thank V. Tidwell, L. C. Meigs, R. M. Holt, S. A. McKenna, A. R. Lappin, and C. F. Harvey for their comments and suggestions. We also appreciate the logistical support of M. J. Kelley. This work was funded by Sandia Corporation, a Lockheed Martin company, for the United States Department of Energy under Contract DE-AC04-94AL85000.

REFERENCES

Armstrong, J. E., Frind, E. O., and McClellan, R. D. 1994. Nonequilibrium mass transfer between the vapor, aqueous, and solid phases in unsaturated soils during vapor extraction. Water Resour. Res. 30(2), 355-368.

Ball, W. P., and Roberts, P. V. 1991. Long-term sorption of halogenated organic chemicals by aquifer material. 2. Intraparticle diffusion. Eviron. Sci. Technol. 25(7), 1237-1249.

Bard, Y. 1974. Nonlinear Parameter Estimation. Academic Press. New York, NY. 341 p..

Bear, J. 1972. Dynamics of Fluids in Porous Media. Dover. New York, NY. 764 p.

Brusseau, M. L., and Rao, P. S. C. 1989. Sorption nonideality during organic contaminant transport in porous media. Crit. Rev. Environ. Control. 19(1), 33-99.

Christian-Frear, T. L., Tidwell, V. C., and Meigs, L. C. 1997. Technical memorandum: Results of experimental methodology development for visualizing and quantifying matrix diffusion in the Culebra Dolomite. NH184. Geohydrology Dept., Sandia National Laboratories. Albuquerque, NM. 28 p.

Culver, T. B., Hallisey, S. P., Sahoo, D., Deitsch, J. J., and Smith, J. A. 1997. Modeling the desorption of organic contaminants from long-term contaminated soil using distributed mass transfer rates. Environ. Sci. Technol. 31(6), 1581-1588.

Cunningham, J. A., and Roberts, P. V. 1998. Use of temporal moments to investigate the effects of nonuniform grain-size distribution on the transport of sorbing solutes. Water Resour. Res. 34(6), 1415-1425.

Cunningham, J. A., Werth, C. J., Reinhard, M., and Roberts, P. V. 1997. Effects of grain-scale mass transfer on the transport of volatile organics through sediments. 1. Model development. Water Resour. Res. 33(12), 2713-2726.

Cussler, E. L. 1976. Multicomponent Diffusion. Elsevier. New York, NY. 176 p.

Cussler, E. L. 1997. Diffusion: Mass Transfer in Fluid Systems. Cambridge University Press. New York, NY. 580 p.

Deans, H. A., and Carlisle, C. T. 1986. Single-well tracer test in complex pore systems. Society of Petroleum Engineers/U.S. Department of Energy SPE/DOE 14886. 61-68.

de Hoog, F. R., Knight, J. H., and Stokes, A. N. 1982. An improved method for numerical inversion of Laplace transforms. SIAM Jour. Sci. Stat. Comput. 3(3), 357-366.

Dykhuizen, R. C., and Casey, W. H. 1989. An analysis of solute diffusion in the Culebra Dolomite. SAND89-0750. Sandia National Laboratories. Albuquerque, NM. 50 p.

Fleming, S. W. 1998. Single and Multiple Rates of Nonequilibrium Diffusive Mass Transfer at the Laboratory, Field, and Regional Scales in the Culebra Member of the Rustler Formation, New Mexico. M.S. thesis, Oregon State University. Corvallis, OR. 172 p.

Fry, V. A., and Istok, J. D. 1994. Effects of rate-limited desorption on the feasibility of in situ bioremediation. Water Resour. Res. 30(8), 2413-2422.

Gierke, J. S., Hutzler, N. J., and McKenzie, D. B. 1992. Vapor transport in unsaturated soil columns: Implications for vapor extraction. Water Resour. Res. 28(2), 323-335.

Goltz, M. N., and Oxley, M. E. 1991. Analytical modeling of aquifer decontamination by pumping when transport is affected by rate-limited sorption. Water Resour. Res. 27(4), 547-556.

Grathwohl, P., and Kleineidam, S. 1995. Impact of heterogeneous aquifer materials on sorption capacities and sorption dynamics of organic contaminants. Groundwater Quality: Remediation and Protection. IAHS. Wallingford, Oxfordshire, England. 79-86.

Haggerty, R., and Gorelick, S. M. 1995. Multiple-rate mass transfer for modeling diffusion and surface reactions in media with pore-scale heterogeneity. Water Resour. Res. 31(10), 2383-2400.

Haggerty, R., and Gorelick, S. M. 1998. Modeling mass transfer processes in soil columns with pore-scale heterogeneity. Soil Sci. Soc. Am. J., 62(1), 62-74.

Haggerty, R., and Harvey, C. F. 1997. A comparison of estimated mass transfer rate coefficients with the time-scales of the experiments from which they were determined. EOS Trans., 78(46), F293.

Haggerty, R., Fleming, S. W., Meigs, L. C., and McKenna, S. A. In review. Convergent-flow tracer tests in a fractured dolomite, 3, Analysis of mass transfer in single-well injection-withdrawal tests. Water Resour. Res..

Harmon, T. C., Semprini, L., and Roberts, P. V. 1992. Simulating groundwater solute transport using laboratory-based sorption parameters. J. Environ. Eng. 118(5), 666-689.

Harmon, T. C., and Roberts, P. V. 1994. Comparison of intraparticle sorption and desorption rates for a halogenated alkene in a sandy aquifer material. Environ. Sci. Technol. 28(9), 1650-1660.

Harvey, C. F., Haggerty, R., and Gorelick, S. M. 1994. Aquifer remediation: A method for estimating mass transfer rate coefficients and an evaluation of pulsed pumping. Water Resour. Res. 30(7), 1979-1991.

Harvey, J. W., Wagner, B. J., and Bencala, K. E. 1996. Evaluating the reliability of the stream tracer approach to characterize stream-subsurface water exchange. Water Resour. Res. 32(8), 2441-2451.

Hollenbeck, K. J., Harvey, C. F., Haggerty, R., and Werth, C. J. 1999. A method for estimating distributions of mass transfer rate coefficients with application to purging and batch experiments. J. Contam. Hydrol. 37(3-4), 367-388.

Holt, R. M. 1997. Conceptual model for transport processes in the Culebra Dolomite Member, Rustler Formation. SAND97-0194. Sandia National Laboratories, Albuquerque, NM.

Kelley, V. A., and Saulnier, G. J., Jr. 1990. Core analyses for selected samples from the Culebra Dolomite at the Waste Isolation Pilot Plant site. SAND90-7011. Sandia National Laboratories, Albuquerque, NM.

Knopman, D. S., and Voss, C. I. 1987. Behavior of sensitivities in the one-dimensional advection-dispersion equation: Implications for parameter estimation and sampling design. Water Resour. Res. 23(2), 253-272.

Lovera, O. M., Richter, F. M., and Harrison, T. M. 1989. The $^{40}Ar/^{39}Ar$ thermochronometry for slowly cooled samples having a distribution of diffusion domain sizes. J. Geophys. Res. 94(B12), 17,917-17,935.

Lovera, O. M., Heizler, M. T., and Harrison, T. M. 1993. Argon diffusion domains in K-feldspar II: Kinetic properties of MH-10. Contrib. Mineral. Petrol. 113(3), 381-393.

Mann, U. 1994. An integrated approach to the study of primary petroleum migration. In Geofluids: Origin, Migration and Evolution of Fluids in Sedimentary Basins, J. Parnell , ed. Geological Society Special Publication No. 78. The Geological Society, London.

Marquardt, D. W. 1963. An algorithm for least-squares estimation of nonlinear parameters. SIAM J.. Indust. Appl. Math. 11(2), 431-441.

McKenna, S. A., Meigs, L. C., and Haggerty, R. In review. Convergent-flow tracer tests in a fractured dolomite, 4, Double porosity, multiple mass-transfer rate processes in two-well convergent flow tests. Water Resour. Res.

Meigs, L. C., and Beauheim, R. L. In review. Tracer tests in a fractured dolomite, 1, Experimental design and observed tracer recoveries. Water Resour. Res..

Ohlsson, Y., and Neretnieks, I. 1995. Literature survey of matrix diffusion theory and of experiments and data including natural analogues. SKB Technical Report 95-12. Swedish Nuclear Fuel and Waste Management Co. Stockholm. 89 p.

Pedit, J. A., and Miller, C. T. 1994. Heterogeneous sorption processes in subsurface systems, 1, Model formulations and applications. Environ. Sci. Technol. 28(12), 2094-2104.

Pedit, J. A., and Miller, C. T. 1995. Heterogeneous sorption processes in subsurface systems, 2, Diffusion modeling approaches. Environ. Sci. Technol. 29(7), 1766-1772.

Pignatello, J. J. 1990. Slowly reversible sorption of aliphatic halocarbons in soils, 2, Mechanistic aspects. Environ. Toxicol. Chem. 9(9), 1117-1126.

Qin, Z., Lu, F., and Anderson, A. T., Jr. 1992. Diffusive reequilibration of melt and fluid inclusions. Am. Mineral.. 77(5-6), 565-576.

Quinodoz, H. A. M., and Valocchi, A. J. 1993. Stochastic analysis of the transport of kinetically sorbing solutes in aquifers with randomly heterogeneous hydraulic conductivity. Water Resour. Res. 29(9), 3227-3240.

Rabideau, A. J., and Miller, C. T. 1994. Two-dimensional modeling of aquifer remediation influenced by sorption nonequilibrium and hydraulic conductivity heterogeneity. Water Resour. Res. 30(5), 1457-1470.

Rao, P. S. C., Rolston, D. E., Jessup, R. E., and Davidson, J. M. 1980. Solute transport in aggregated porous media: Theoretical experimental evaluation. Soil Sci. Soc. Am. J. 44(6), 1139-1146.

Roberts, P. V., Goltz, M. N., and MacKay, D. M. 1986. A natural gradient experiment on solute transport in a sand aquifer. 3. Retardation estimates and mass balances for organic solutes. Water Resour. Res. 22(13), 2047-2058.

Rügner, H., Kleineidam, S., and Grathwohl, P. 1999. Long term sorption kinetics of phenanthrene in aquifer materials. Environ. Sci. Technol. 33(10), 1645-1651.

Ruthven, D. M., and Loughlin, K. F. 1971. The effect of crystalline shape and size distribution on diffusion measurements in molecular sieves. Chem. Eng. Sci. 26(5), 577-584.

Satterfield, C. N., Colton, C. K., and Pitcher, W. H., Jr. 1973. Restricted diffusion in liquids within fine pores. AIChE J. 19(3), 628-635.

Shackelford, C. D. 1991. Laboratory diffusion testing for waste disposal - A review. J. Contam. Hydrol. 7(3), 177-217.

Steinberg, S. M., Pignatello, J. J., and Sawhney, B. L. 1987. Persistence of 1,2-dibromoethane in soils: Entrapment in intraparticle micropores. Environ. Sci. Technol. 21(12), 1201-1208.

Tidwell, V. C., and Glass, R. J. 1994. X ray and visible light transmission for laboratory measurement of two-dimensional saturation fields in thin-slab systems. Water Resour. Res., 30(11), 2873-2882.

Tidwell, V. C., Meigs, L. C., Christian-Frear, T., and Boney, C. M. In press. Effects of spatially heterogeneous porosity on matrix diffusion as investigated by X-ray absorption imaging. J. Contam. Hydrol.

Tomich, J. F., Dalton, R. L., Jr., Deans, H. A., and Shallenberger, L. K. 1973. Single-well tracer method to measure residual oil saturation. J. Petrol. Technol., 25(2), 211-218.

Villermaux, J. 1981. Theory of linear chromatography. Percolation Processes: Theory and Applications. A. E. Rodrigues and D. Tondeur, eds. Sijthoff & Noordhoff. Rockville, MD. NATO ASI Ser. E. 33, 83-140.

Welty, J. R., Wicks, C. E., and Wilson, R. E. 1984. Fundamentals of Momentum, Heat, and Mass Transfer. John Wiley and Sons. New York, NY. 803 p.

Werth, C. J., Cunningham, J. A., Roberts, P. V., and Reinhard, M. 1997. Effects of grain-scale mass transfer on t he transport of volatile organics through sediments. 2. Column results. Water Resour. Res. 33(12), 2727-2740.

Wood, W. W., Kraemer, T. F., and Hearn P. P., Jr. 1990. Intragranular diffusion: An important mechanism influencing solute transport in clastic aquifers? Science. 247(4950), 1569-1572.

TABLE CAPTIONS

Table 1: Brief descriptions of Culebra dolomite samples used in the static diffusion experiments, including bulk porosity (adapted from *Christian-Frear et al., 1997* and *Tidwell et al., in press*).

Table 2: Results for single-rate and multirate parameter estimations. D_p is the best-fit pore diffusivity estimated using a conventional single-rate model. Values of μ_d and σ_d are best-fit parameters of the lognormal distribution of pore diffusivity used in the multirate inversion. The value μ_d may be compared to $\ln(D_p)$. Quality of the fits to the data are described by the log-space root mean square errors for both single-rate (SR) and multirate (MR) inversions. Out-diffusion experiments were not conducted for samples RC4-D and RC6-G.

FIGURE CAPTIONS

Figure 1: Location map.

Figure 2: Scales and types of Culebra matrix porosity (from *Holt, 1997*).

Figure 3: Mass uptake and recovery data. Figure 3.a: in-diffusion. Vertical axis gives the value of $1-M(t)/M(t=\infty)$. Figure 3.b: out-diffusion. Vertical axis gives $M(t)/M(t=0)$. Out-diffusion experiments were not conducted for samples RC4-D and RC6-G.

Figure 4: Empirical and best-fit CDFs of formation factor. Data is for Culebra samples analyzed by TerraTek (*Holt, 1997*). Samples were taken from the H-19 hydropad, primarily borehole H-19 b4 (*R. Beauheim, personal communication, 1997*); samples used in static diffusion experiments were taken from the same location. Best-fit lognormal CDF was determined by manual calibration and has a geometric mean of 4.5 (corresponding to a formation factor of 90) and a standard deviation of 0.7. Earlier work at other locations at the WIPP site by *Kelley and Saulnier (1990)* also suggests that formation factors in the Culebra dolomite are lognormally distributed. Formation factors are commonly taken to be inversely proportional to diffusivity (*e.g., Bear, 1972; Kelley and Saulnier, 1990*), so reasonably good quality of the fit suggests that use of a lognormal distribution to approximate the true distribution of D_p in the Culebra is appropriate. Calculations of D_p from formation factors tend to be unreliable, due to the dependence of formation factor measurements on the properties of the ions present in the pore fluid and uncertainty in the precise form of the relationship between formation factor and D_p (see *Kelley and Saulnier, 1990* for discussion). However, the standard deviation of the lognormal distribution of formation factors should be a good approximation to σ_d in the distribution of D_p.

Figure 5: Sensitivity analysis. Forward simulations were performed for the case of in-diffusion. Vertical axis on both plots gives the value of $1-M(t)/M(t=\infty)$. Figure 5.a: model responses for three values of μ_d, holding σ_d constant at 1. Units of μ_d are hr^{-1}. Figure 5.b: model responses for three values of σ_d, holding μ_d constant at –13; note that $\sigma_d=0$ corresponds to a conventional single-rate model. The effects of variation in σ_d are far more pronounced at late times and for small values of the mass ratio, relative to the effects of variation in μ_d.

Figure 6: Mass ratio data and model responses. Best-fit curves were calculated using both a conventional single diffusivity (single-rate model) and a lognormal distribution of diffusivities (multirate model). Figure 6.a: in-diffusion for sample RC1-A. Vertical axis gives the value of $1-M(t)/M(t=\infty)$. Figure 6.b: out-diffusion for bulk data. Vertical axis gives the value of $M(t)/M(t=0)$.

Sample	θ	L (cm)	Description
B33-H	0.15	5.5	Abundant open vugs directly interconnected and/or interconnected by fractures; some gypsum-filling of vugs. Major porosity types = intercrystalline, vugs, and fractures.
RC1-A	0.13	4.9	Relatively uniform; single faint lamina; minor microvugs and (?)microfractures. Major porosity types = intercrystalline.
RC2-B	0.09	6.6	Distinct fracture spanning half the length of the sample. Major porosity types = Intercrystalline and fractures.
RC4-D	0.09	5.8	Faint laminations; minor vuggy porosity scattered throughout; minor microfractures. Major porosity types = intercrystalline.
RC6-G	0.12	6.2	Abundant large (0.025 to 2.0 cm) vugs; abundant fractures; considerable gypsum-filling of fractures and vugs. Major porosity types = intercrystalline, fractures, and vugs.

Table 1

Test	D_p [m²/hr] *$ln(D_p) \pm 2\sigma$* range	$\mu_d \pm 2\sigma$ range	σ_d *$ln(\sigma_d) \pm 2\sigma$* range	$RMSE_{SR}$	$RMSE_{MR}$
B33-H in	4.78E-06 *-12.2 ± 0.230* 3.80E-06, 6.02E-06	-12.0 ± 0.242 -11.8, -12.2	0.598 *-0.514 ± 0.0610* 0.563, 0.636	0.730	0.510
B33-H out	2.64E-06 *-12.8 ± 1.15* 8.74E-07, 8.72E-06	-11.7 ± 3.14 -8.56, -14.8	0.946 *-0.0555 ± 2.12* 0.114, 7.88	5.78	3.01
RC1-A in	1.22E-06 *-13.6 ± 0.196* 1.00E-06, 1.51E-06	-13.5 ± 0.344 -13.2, -13.8	0.958 *-0.0429 ± 0.892* 0.393, 2.34	0.245	0.169
RC1-A out	4.96E-07 *-14.5 ± 0.178* 4.22E-07, 6.03E-07	-14.5 ± 0.276 -14.2, -14.8	0.560 *-0.580 ± 1.73* 0.0997, 3.16	0.218	0.163
RC2-B in	1.49E-06 *-13.4 ± 0.195* 1.25E-06, 1.84E-06	-13.4 ± 0.334 -13.1, -13.7	0.666 *-0.407 ± 2.08* 0.0832, 5.33	0.161	0.157
RC2-B out	1.30E-06 *-13.6 ± 0.161* 1.06E-06, 1.46E-06	-13.5 ± 0.240 -13.3, -13.7	0.00590 *-5.13 ± 2.22E+04* 0.00, ∞	0.275	0.274
RC4-D in	9.75E-07 *-13.8 ± 0.340* 7.23E-07, 1.43E-06	-13.9 ± 0.622 -13.3, -14.5	0.988 *-0.0121 ± 2.06* 0.126, 7.75	0.241	0.239
RC6-G in	3.66E-06 *-12.5 ± 0.274* 2.83E-06, 4.90E-06	-12.5 ± 0.496 -12.0, -13.0	0.0369 *-3.30 ± 472* 0, ∞	0.516	0.517
Bulk in	2.15E-06 *-13.1 ± 0.198* 1.68E-06, 2.49E-06	-13.0 ± 0.194 -12.8, -13.2	0.976 *-0.0243 ± 0.0178* 0.959, 0.994	0.253	0.152
Bulk out	1.15E-06 *-13.7 ± 0.496* 6.84E-07, 1.84E-06	-13.2 ± 0.552 -12.6, -13.8	1.20 *0.182 ± 0.652* 0.625, 2.30	1.02	0.495

Table 2

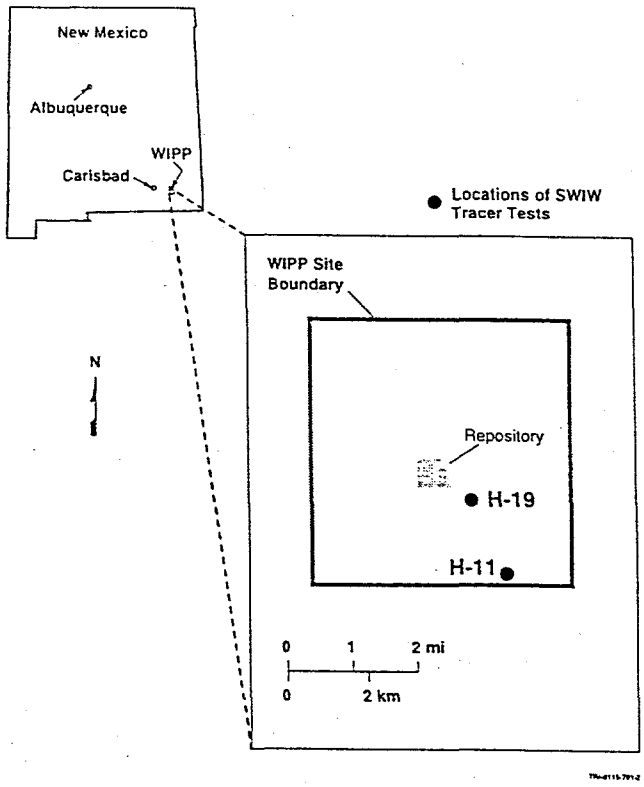
New Mexico
Albuquerque
WIPP
Carlsbad
Locations of SWIW Tracer Tests
WIPP Site Boundary
N
Repository
H-19
H-11
0 1 2 mi
0 2 km

Figure 1

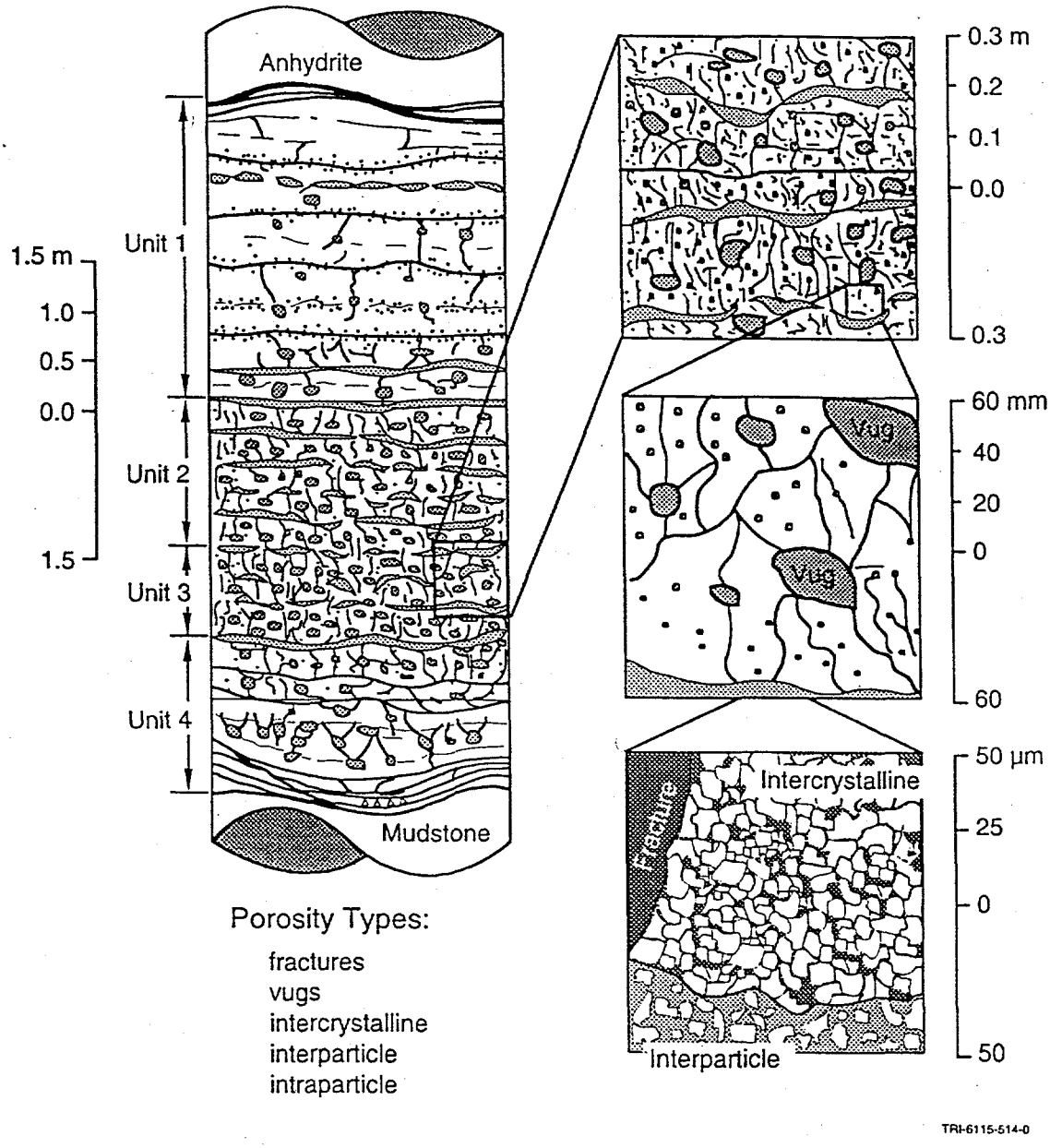
Anhydrite
Unit 1
Unit 2
Unit 3
Unit 4
Mudstone
1.5 m
1.0
0.5
0.0
1.5
0.3 m
0.2
0.1
0.0
0.3
60 mm
40
20
0
60
Vug
Vug
50 µm
25
0
50
Fracture
Intercrystalline
Interparticle
Porosity Types:
fractures
vugs
intercrystalline
interparticle
intraparticle
TRI-6115-514-0

Figure 2

Figure 3.a

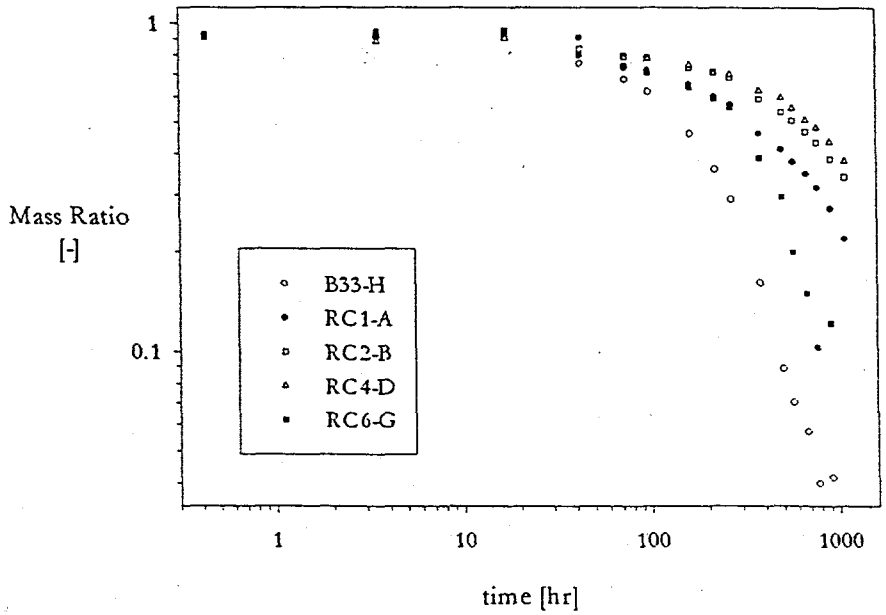

Figure 3.b

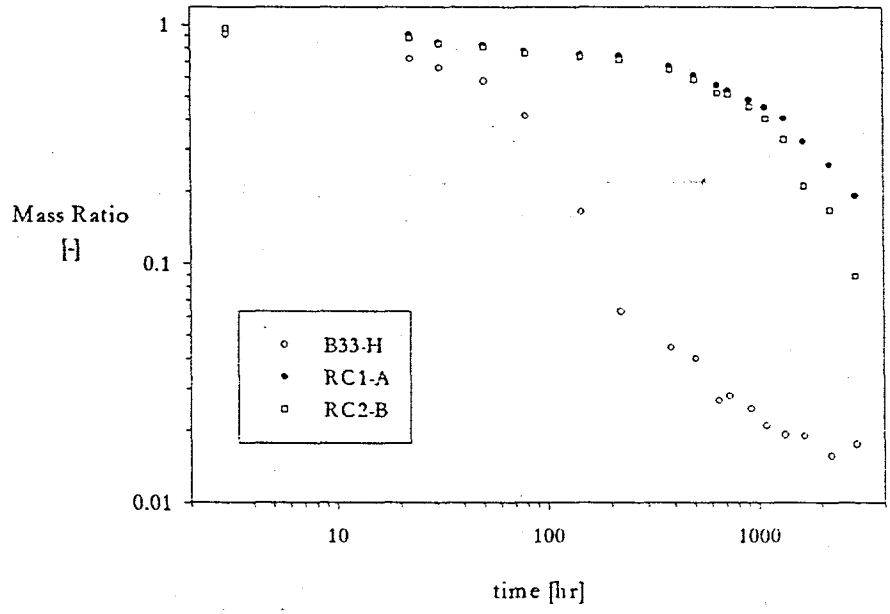

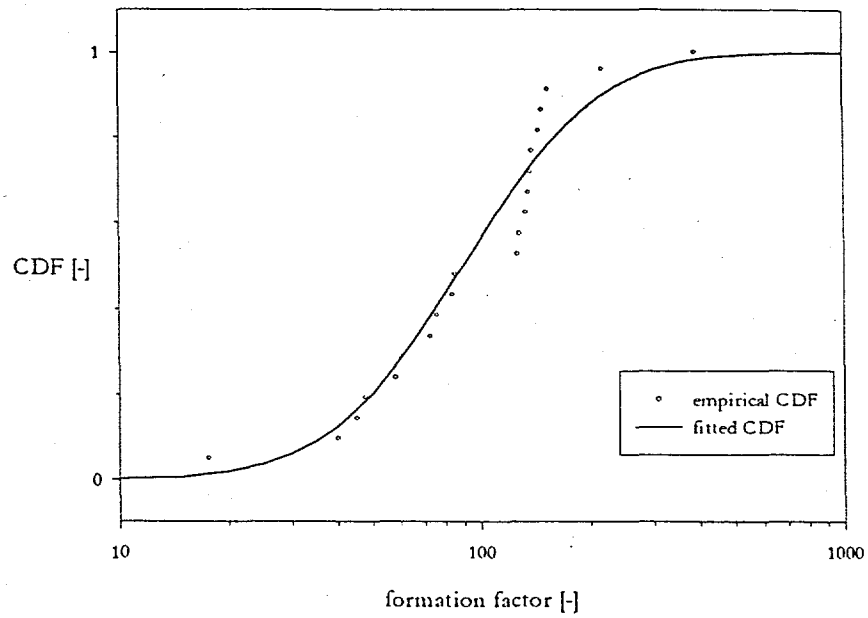
1
0
CDF [-]
10
100
1000
formation factor [-]
empirical CDF
fitted CDF

Figure 4

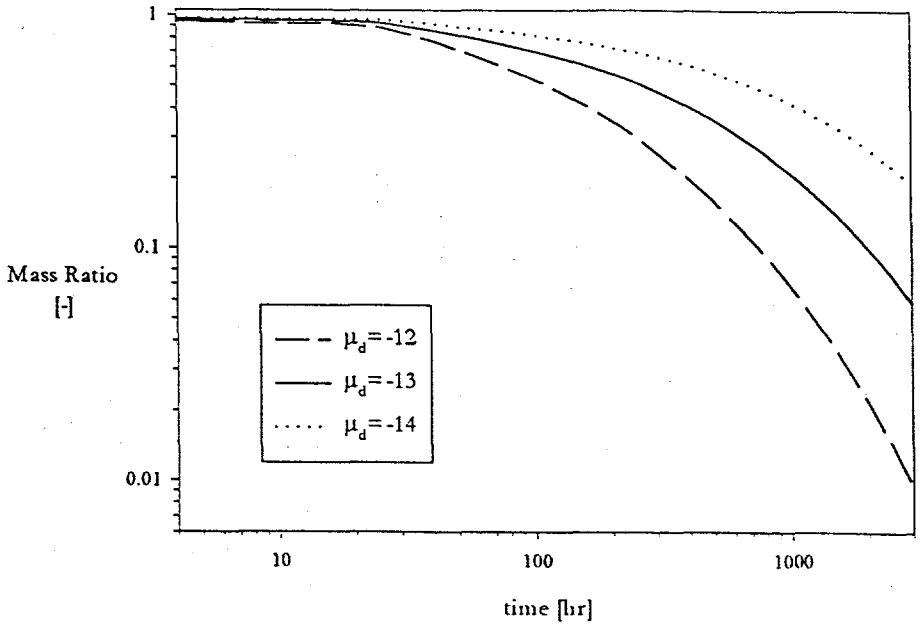

Figure 5.a

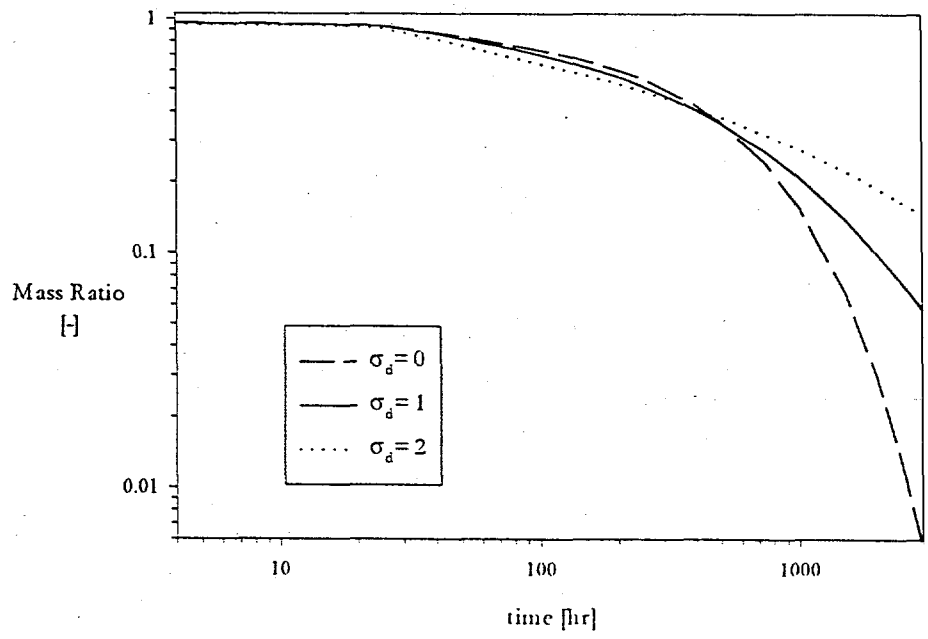

Figure 5.b

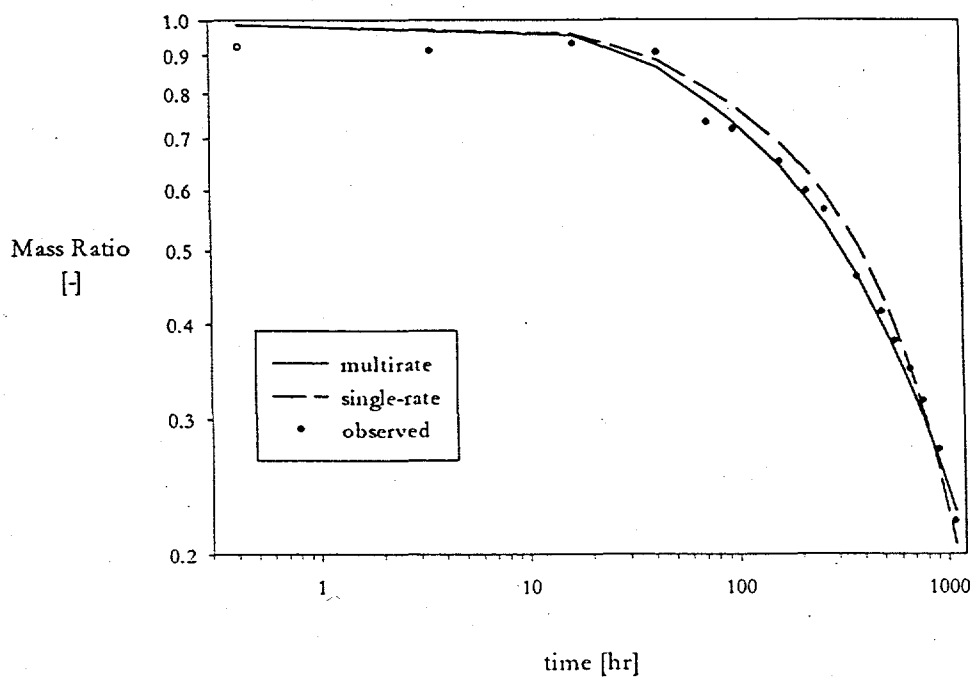
1.0
0.9
0.8
0.7
0.6
0.5
0.4
0.3
0.2
Mass Ratio
[-]
multirate
single-rate
observed
1
10
100
1000
time [hr]

Figure 6.a

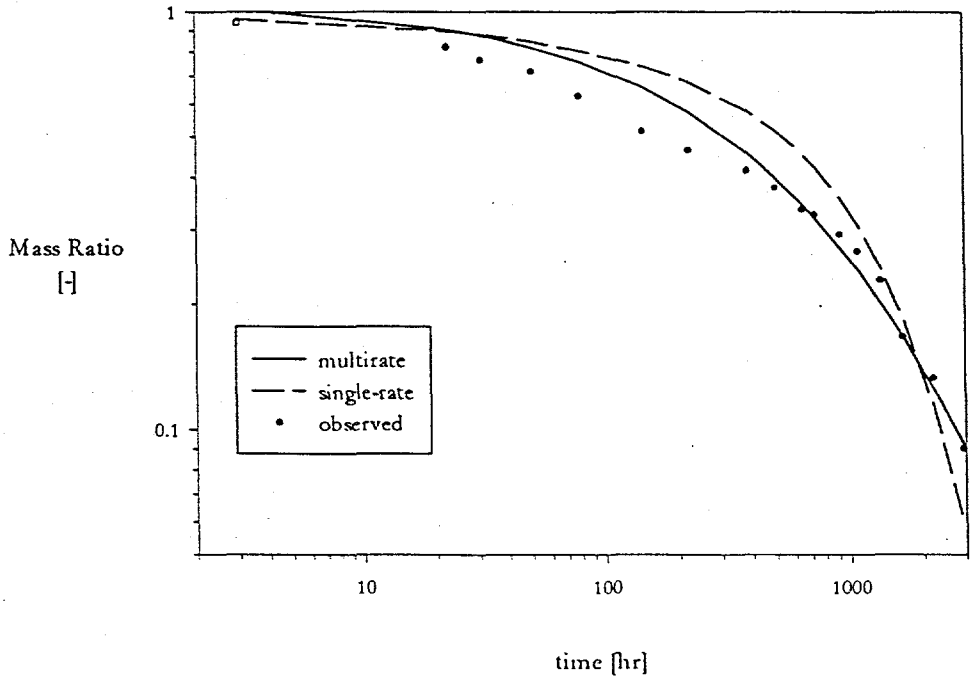
Mass Ratio
[-]
1
0.1
multirate
single-rate
observed
10
100
1000
time [hr]

Figure 6.b